DIRECTIONS FOR IMPROVING PPT PERFORMANCE

P.J. Turchi

The Ohio State University
Columbus, Ohio USA

ABSTRACT

Potential improvements in PPT performance are discussed from analytical considerations, and comprise the following sequence of conditions that need to be established. Presently, the exhaust of the PPT is allowed to expand without regard to extracting directed kinetic energy efficiently from the hot, highly-magnetized plasma in the thrust chamber. Analytically, it appears that improvements by a factor of 1.7 in specific impulse and three in thrust efficiency should be possible with proper expansion. A major area for improving PPT performance is the reduction of relative mass expelled that is not electromagnetically-accelerated to high speed. Analytical modeling indicates that mass evolved by post-discharge evaporation can exceed that during the discharge by a factor of more than five. An inductively-driven circuit, previously suggested, would maintain electromagnetic acceleration as the propellant surface cools. This circuit also improves PPT performance by eliminating losses and difficulties of present oscillatory waveforms.

INTRODUCTION

It is useful to consider directions for improving the pulsed plasma microthruster (PPT) so that it may be applied to a greater range of missions. In particular, higher thrust efficiency, and, for some uses, higher specific impulse are needed. It is critical that improvements to the PPT retain the simplicity that allowed its early operation in actual space missions, and maintain the connection to the PPTs extensive flight-experience. Of the four or five devices selected from dozens of concepts in electric propulsion, only the PPT has both a record of actual accomplishment in space, and the potential for significant improvement through further research. The other devices have already been taken to high levels of performance (probably their limiting values) by many years of sustained laboratory research and development.

BASIC OPERATION OF PRESENT PPT

The traditional pulsed plasma microthruster (PPT) operates with an unsteady, oscillatory discharge. This is a consequence of the relatively low energies used by PPTs for satellite station-keeping. With a stored-energy in the capacitor on the order of 20 J, at an initial voltage of 2 kV, the capacitance is only 10 µf.; circuit inductance values below 100 nh are difficult to obtain with commercially-available components. The impedance of an LRC-circuit for critical damping is $2(L/C)^{1/2} = 200$ mΩ. The characteristic impedance of the electromagnetically-accelerated discharge flow, however, is (for a propagating discharge, with inductance gradient, L'):

$$Z_d = L' u / 2 \qquad (1)$$

so, at an exhaust speed of 40 km/s, and L' = 10^{-6} h/m, $Z_d = 20$ mΩ. Thus, the circuit is hardly loaded by the thruster, and can deposit much of its energy in the internal resistance of the capacitor. The losses associated with such resistance increases the operating temperature of the capcacitor. The combination of higher temperature with the severe and repeated reversals of the capacitor voltage reduces the reliable life of the capacitor, which must be compensated by a reduction in design voltage and energy per unit mass.

It is also typical of traditional PPT operation that the discharge flow simply exits abruptly from a constant area. For a magnetized-plasma flow, this fails to extract energy from the magnetic field (and any accessible thermal modes) into the directed kinetic energy of the exhaust. An additional source of inefficiency in traditional PPTs has recently been suggested after initial attempts at numerical simulation of the LES-6 device[1]. The numerical calculations, using the MACH2 code, agreed well with the impulse-bit per shot, but the mass ablated during the discharge pulse was about a factor of ten lower in the simulation vs the experimental data for mass loss per shot. Subsequent calculation indicated that evaporation of the Teflon propellant between firings might account for this mass discrepancy. If a major portion of the mass per shot is lost at relatively low speed, then the efficiency of the PPT is substantially reduced from ideal values.

In combination, the efficiency factors associated with external-circuit resistance (<60%), improper flow expansion (<33%) and mass loss at low speed (<50%) multiply to provide a total thruster efficiency of less than 10% . By addressing each of the inefficiencies in turn, it should be possible to improve the performance of the PPT substantially.

Consideration may be framed first in terms of quasi-analytical modeling, before invoking more powerful numerical tools and testing ideas experimentally. Idealized modeling may be applied to initial design of proper flow expansion, to the questions of mass loss and thermal management and, finally, to improved circuitry for the PPT.

IDEALIZED MODEL FOR PPT

The essential features of the ablation-fed discharge in the PPT include resistive heating near the entrance of a constant-area channel (where the back EMF is relatively low), heat transfer from the discharge back to the propellant surface to provide mass by ablation, and electromagnetic acceleration of the plasma by the Lorentz force. In pulsed operation, particularly with high-frequency, oscillatory waveforms, the preceding features are unsteady and require numerical modeling for accurate calculations in time and space. A first step in simplifying analysis of the PPT, while attempting to retain the fundamental interactions among resistive heating, heat transfer and flow, restricts examination to a steady state, and one-dimensional flow. (The details of such examination are briefly described in Appendix I.) The use of a steady analysis in discussing the PPT, however, means that comments can only be applied to situations in which there is enough time for the discharge flow to operate with a balance of heat conduction, resistive dissipation and flow acceleration. Convective times based on the discharge thickness divided by the flow speed must certainly be less than the time for variation of circuit current. Furthermore, the ablating surface must be able to supply new material in times shorter than the convective time. Thus, for example, discharges that lift off of refractory insulators may remain in an unsteady, propagating mode, rather than achieving the quasi-steady situation of the present analysis.

For a Teflon-based PPT, the analysis of Appendix I suggests that an ablation arc, with a thickness less than two millimeters, is formed adjacent to the propellant surface. In the numerical example, the speed of the flow through the arc increases by a factor of about three to an exit velocity of 41 km/s. The characteristic convective time for the flow structure is therefore about 0.1 μsec. Heat conduction to the colder upstream boundary automatically supplies the power needed to dissociate and ionize the flow, and also the relatively minor, additional power level required to provide mass flow by ablation. The calculated size and timescale suggest that the analysis is consistent with PPT operation at frequencies (within the discharge pulse) less than a MHz, and dimensions greater than a cm.

SPECIFIC IMPULSE

As previously noted in a simpler analysis (without heat conduction)[2], the proportionality of resistive heating and electromagnetic work, in the context of a flow in which heat is largely absorbed by the ionization of the propellant, leads to an exhaust speed that scales closely with Alfven critical speed. Thus, the specific impulse of self-field, plasma thrusters, operating with mass addition (vs constant mass, propagating discharges) will tend to values proportional to Alfven critical speed, if heating can supply additional conducting material. Improvements of PPT performance, in terms of higher specific impulse, therefore, would require propellants with lower average molecular-mass than the Teflon presently used. In the present example, the computed exit speed already corresponds to a specific impulse of 4180 s. Even moderate attention to proper expansion of this magnetosonic flow to magnetic field-free conditions will offer values of specific impulse that cover the range of any near term missions, (upwards of 7000 s). The earlier analysis[2] suggests improvements by up to $3^{1/2}$. The principal reason for the more modest values of specific impulse (~ 1000 s) is mass that is not accelerated electromagnetically (e.g., post-discharge evaporation).

MASS ABLATED DURING DISCHARGE

By the analysis of Appendix I, the necessary mass-flow rate is actually controlled by a magnetosonic condition in the constant-area channel, rather than a separate condition on heat transfer to the propellant surface. The details of such heat transfer adjust to satisfy the mass flow constraints in the overall MHD flow. The mass loss during the discharge pulse may thus be estimated from the mass flow rate (per unit area):

$$w = \rho^* u^* \qquad (2)$$

where the speed at the sonic point is:

$$u^* = \{(B^{*2} / \rho^* \mu)[1 + \gamma \beta^* / 2]\}^{1/2} \qquad (3)$$

and the mass density there is:

$$\rho^* = (\beta^* B^{*2} / 2\mu) / R^* T^* \qquad (4)$$

The temperature at the sonic point is obtained in terms of the magnetic field at the propellant surface, B_1:

$$T^* = \{ \Lambda / f_1 \mu (K_h / K_r)^{1/2} \}^{2/5} B_1^{2/5} \qquad (5)$$

The mass flow rate is therefore proportional to $B_1^{9/5}$. For a constant current, the mass ablated during a pulsetime t_p is merely wAt_p, where A is the area of the ablating surface. In the case of an exponentially-decaying sinusoidal pulse, within the quasi-steady approximation, the mass flow rate may be integrated over the oscillatory waveform; if the ratio of risetime to decay time is 0.3, for example, the mass ablated is $0.933w_0At_r$, where t_r is the risetime and w_0 is the mass flow rate per unit area based on the undamped amplitude of the current. Note that this represents a nearly linear dependence on stored energy, W_0, in the capacitor ($\Delta m \sim W_0^{9/10}$) for the mass ablated during the discharge.

THERMAL CONDITIONS AT SURFACE

The mass lost between discharges may be considered in terms of the temperature of the propellant surface. From the idealized analysis, it is possible to estimate the surface temperature of the propellant that is consistent with the flow conditions. In particular, the equibrium vapor pressure should equal the total pressure at the entrance to the ablation arc. A formula for the equilibrium vapor pressure for Teflon is:

$$P_{eq} = p_c \exp (- T_c / T) \qquad (6)$$

with $T_c = 20{,}815$ K and $p_c = 1.872 \times 10^{20}$ N/m^2.

The total pressure calculated from the one-dimensional, idealized model is:

$$P_t = p_1 + \rho_1 u_1^2 \qquad (7)$$

$$= (B_1^2 / 2\mu f_1^2) [\beta^* \theta_1/\omega_1$$
$$+ (2 + \gamma\beta^*)\omega_1]$$

The necessary surface temperature is then:

$$T_s = T_c / \ln \{ p_c / (B_1^2 / 2\mu f_1^2)[\beta^* \theta_1/\omega_1$$
$$+ (2 + \gamma\beta^*)\omega_1]\} \qquad (8)$$

For the numerical example of Appendix I, the surface temperature is 600 K. Note: this value is only weakly dependent on the operating magnetic field, but material transitions can be quite sensitive to exact values of temperature. This particular value is very close to the melting point of Teflon (~ 600 K). (Nonuniformities in arc distribution across the face of the propellant might cause local melting in any event.) The depth of propellant heated to this temperature during pulsetimes of several microseconds is less than a few microns. Growth of

perturbations of a liquefied surface due to Rayleigh-Taylor instability would be suppressed for wavelengths approaching the depth of the layer, while the exponential growth of shorter wavelengths would not persist beyond amplitudes comparable to these wavelengths. Thus, micron-size droplets might be expected, especially from edges. Such droplets would be responsible for mass loss by surface disruption, as indicated in some experiments[3].

THERMAL MANAGEMENT

It has been suggested[1] that the loss of mass between shots depends critically on the overall thermal management of the PPT, both in the laboratory and in space. The estimated surface temperature is well above mean-values within the propellant measured in laboratory tests[4] at total power levels of 40 W (40 J at 1 Hz) which indicate a rise over several thousand shots from room temperature (300 K) to about 370 K. For the acknowledged low efficiency of present PPT operation, only a small fraction of the total power is delivered to the Teflon surface. The estimated surface temperature allows calculation of the heat deposited in the surface during the pulse, based on the thermal skin-depth , δ:

$$H = \rho c A\delta (T_s - T_i) \qquad (9)$$

where the thermal skin-depth is given in terms of the pulsetime t_p as:

$$\delta = (k\, t_p / \rho c)^{1/2} \qquad (10)$$

With $k = 0.305$ W/m-s-K, $\rho = 2.15 \times 10^3$ kg/m^3, and $c = 1171$ J/kg, a pulsetime of 10 μs would provide a skin-depth of 1.1 microns. At a surface temperature of 600 K, this contains 637 J/m^2 of heat added by the discharge pulse, which represents an average heat load to a 4 cm^2 surface of 0.25 W at a 1 Hz repetition rate. This exceeds the power required to evaporate Teflon from the surface by a factor of 5 (using the mass flow computed in Appendix I and a heat of vaporization and de-polymerization of 3.67 MJ/kg). The "extra" power delivered to the surface has consequences for both late-time pulsed and steady mass evolution.

After the discharge pulse ends, the heat deposited in the skin-layer will be shared with the rest of the solid propellant in a depth that continues to increase as the square-root of time. Without further heat addition (or significant cooling due to ablation), the surface temperature will decrease inversely with this depth:

$$(T_s - T_b) / (T_{si} - T_b) = (t_p / t)^{1/2} \qquad (11)$$

where T_{si} is the surface temperature at the end of the discharge pulse ($t = t_p$), and T_b is the base temperature of the propellant. The mass evaporated as the surface cools (for $t > t_p$) may be estimated using this time-dependence of the surface temperature in Eqn. 6.

By assuming one-dimensional expansion of the surface vapor to a (thermally) sonic condition, the mass flow per unit area is:

$$w = (\gamma / 2)[2/(\gamma + 1)]^{1/2} p_s / (\gamma RT_s)^{1/2} \qquad (12)$$

Integration of this mass flow rate provides a total evaporated mass (for $t > t_p$), Δm_e, that is proportional to the magnetic pressure and the pulsetime, allowing comparison with the mass ablated, Δm_d , during the discharge pulsetime:

$$\Delta m_e / \Delta m_d = K\{1 - \exp(-T_c / T_b) / \exp(-T_c / T_{si})\}$$

$$\overline{(T_c / T^*)^{1/2} (T_c / T_{si})^{1/2} (1 - T_b / T_{si})[\beta^*(1 + {}^Y\beta^*/2)(\gamma + 1)/ 4\gamma]^{1/2}}$$

$$(13)$$

For the conditions of the previous numerical example, a base temperature T_b = 370 K, and the factor K = 1.26, the ratio of mass evaporated as the surface cools to that ablated during the discharge pulse is 5.1 . This ratio decreases to 4.3, if the base temperature of the propellant is kept at 300 K, indicating improved performance of PPTs with better cooling. The ratio increases largely as $B_1^{1/5}$, due to the variation of T^*, and thus is rather insensitive to the amplitude of the circuit current. Longer pulsetimes increase the mass ablated during the discharge, but also increase the heat deposited in the solid propellant, which maintains the surface temperature for a longer time after the pulse, allowing significant evaporation to continue longer. Major improvements will require either optimization of material properties or matching of the power circuit to the ablation process to avoid evolution of mass when electromagnetic forces are absent.

QUASI-STEADY, INDUCTIVE OPERATION

One approach to preventing such evolution would reduce the surface temperature needed to support the mass flow through the discharge as thermal conduction into the solid cools the surface. After an initial pulsetime due to the current rise, t_p = t_r, the surface temperature would then decline according to Eqn.11, if no significant additional heat deposition is required in order to supply mass flow to the discharge. Now, let the current decrease so that

the required temperature follows the decreasing temperature of the surface:

$$J / J_0 = B_1 / B_{10}$$
$$= \exp[-(T_c / T_b) / (1 + (T_{si} / T_b - 1)(t_p / t)^{1/2}]$$
$$/ \exp[-(T_c / T_b) / (1 + (T_{si} / T_b - 1)]$$

$$(14)$$

This is displayed in Fig. 1 with t in units of the risetime, $t_r = t_p$. (Temperature values are the same as in the earlier discussion.) Such a waveform may be compared with the experimental current behavior (Fig 2) obtained with an inductively-driven circuit[5] in which a plasma discharge (in this case a second PPT) is used to crowbar the capacitor shortly after peak current.
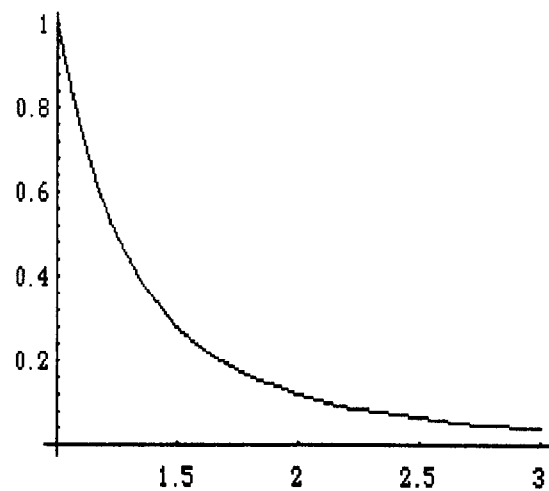
Figure 1: Normalized current waveform, J / J_0 vs time in units of risetime, t / t_r
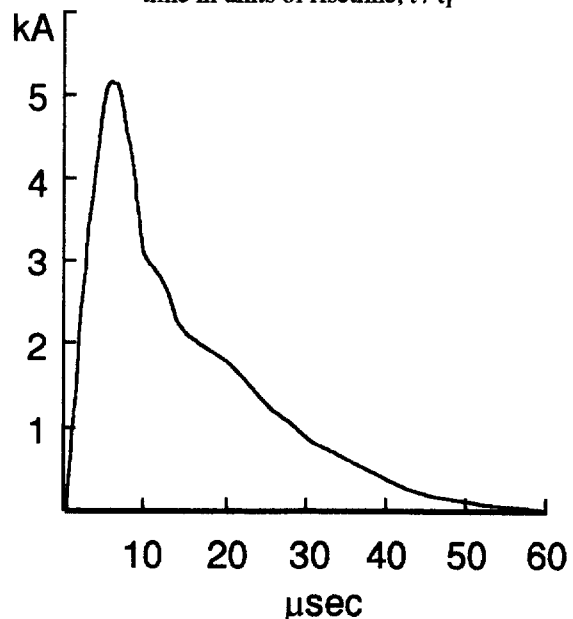
Figure 2: Experimental current waveform for inductively-driven circuit driving PPTs

The use of a inductively-driven circuit not only provides a current waveform that might alleviate mass evolution after the current pulse, but also avoids the severe voltage-reversals on the capacitor. With some attention to reducing the resistance of the external circuit to a small fraction of the PPT impedance, the electrical efficiency should greatly improve. From the idealized analysis, the impedance of the PPT is:

$$Z = u^* B^* h / J \qquad (15)$$

where h is the length of the discharge. For the values previously used, and h = 2 cm, Z = 33 mΩ. At J_0 = 10 kA, and an initial circuit energy of 20 J, the inductance of the store could be 400 nh, for which the characteristic decay time of the waveform would be 12 μsec; the capacitance at an initial voltage of 2 kV is 10 μf, so the risetime is about 3.1 μsec.

CONCLUDING REMARKS

The idealized analysis has indicated that evolution of mass after the discharge pulse is a fundamental consequence of creating mass by ablation during the discharge. It is therefore useful to maintain electromagnetic forces while the surface cools. This can be accomplished simply by means of an inductively-driven circuit, which merely involves placing a low impedance across the energy-storage capacitor shortly after peak current. Such a circuit was originally suggested[5] to improve PPT design by allowing high energy per unit mass at low total energies (without the difficulties of parasitic inductance and internal resistance in the capacitor). In addition to reducing internal losses, reduction of the amplitude of voltage-reversal on the capacitor improves reliability at high energy density. Furthermore, the new circuit provides longer discharge times, so that proper flow expansion techniques can be used; nozzle sizes divided by flow speeds require quasi-steady currents for several μsec.

While the idealized analysis can guide general considerations, and may closely match experimental data in some cases, accurate analysis requires numerical tools, such as MACH2. This includes design of a properly expanded PPT flow, which has recently been successfully attempted with an annular PPT exiting to a plug nozzle.

ACKNOWLEDGEMENTS

REFERENCES

1. P.G. Mikellides and P.J. Turchi, "Modeling of Late-time Ablation in a PPT", AIAA 96-2733.

2. P.J. Turchi and P.G. Mikellides, "Modeling of Ablation-Fed Pulsed Plasma Thrusters", AIAA 95-2915.

3. G. Spanjers, et al, "Power Level Effects and Propellant Losses in a PPT", AIAA 97-2920.

4. H. Kamhawi and P.J. Turchi, "PPT Thermal Management", IEPC 97-125.

5. P.J. Turchi, et al, "Design of an Inductively-Driven Pulsed Plasma Thruster", AIAA 96-2731. Also, H. Kamhawi, for recent experimental data.

A1. L. Spitzer, Physics of Fully Ionized Gases, Wiley (1964). Chapter 5.

APPENDIX I

ONE-DIMENSIONAL, STEADY PLASMA THRUSTER FLOW WITH HEAT CONDUCTION

The conservation equations for a one-dimensional, steady plasma flow with resistive heating and heat conduction are written as:

Mass-flow :

$$\rho u = constant = w \qquad (A1)$$

where ρ is the local mass density and u is the local flow speed. The constant may be evaluated in terms of values at a particular location, $w = \rho^* u^*$.

Momentum :

$$\rho u \frac{du}{dx} + \frac{d}{dx}(B^2/2\mu + p) = 0 \qquad (A2)$$

so,

$$wu + B^2/2\mu + p = constant$$

$$= \rho^* u^{*2} + B^{*2}/2\mu + p^* \qquad (A3)$$

where B is the local magnetic field and p is the local pressure; starred quantities are evaluated at the same location. For simplicity, the pressure may be written as:

$$p = \rho RT \qquad (A4)$$

where T is the local temperature, and R is an appropriate gas constant. The momentum equation then becomes:

$$wu + B^2/2\mu + wRT/u$$

$$= \rho^* u^{*2} + B^{*2}/2\mu + \rho^* R^* T^* \qquad (A5)$$

The temperature distribution depends on the interplay of convection, heat conduction, resistive dissipation, and work, which may be written in terms of the third conservation equation:

Energy :

$$w \frac{dU}{dx} = \frac{d}{dx} k \frac{dT}{dx} + \eta j^2 - p \frac{du}{dx} \qquad (A6)$$

where U is the energy per unit mass, k is the thermal conductivity, η is the electrical resistivity, and j is the current density. In steady state, and one-dimension, the resistive dissipation may be written in terms of an electric field that is uniform:

$$E = \eta j - u \times B + (j \times B - \mathbf{grad}\ p_e) / n_e e \qquad (A7)$$

$$= \text{constant} = E^* \qquad (A8)$$

where the electric field can be evaluated at the starred location for which $j = j^*$, so $E^* = \eta^* j^* + u^* B^*$. (Note that the gradient of the electron pressure, p_e, divided by the electron density, n_e, does not contribute to ηj^2 in the one-dimensional problem, nor does the Hall effect term.) The energy equation is then given by:

$$w \frac{dU}{dx} = \frac{d}{dx} k \frac{dT}{dx} + \frac{(E^*- uB)}{\eta} - p \frac{du}{dx} \qquad (A9)$$

In general, solution of this equation can be accomplished if the detailed behaviors of the energy and pressure functions, and the transport coefficients, k and η, are known in terms of temperature and density.

For ideal plasmas[A1], the thermal conductivity and electrical resistivity can be written in terms of formulas that only involve the temperature, if the plasma is sufficiently ionized (and does not change its degree of ionization) and magnetic fields do not suppress the electron heat conduction unduly. Thus,

$$k = K_h T^{5/2} \quad \text{and} \quad \eta = K_r / T^{3/2} \qquad (A10)$$

where K_h and K_r are constants. (We have also ignored the variation of the Coulomb logarithm here for continued simplicity.)

To delineate the flow structure, and avoid losing general results in consideration of particular plasma values, it is useful to non-dimensionalize variables in terms of conditions at the starred location

(which might later be identified as a sonic point). Thus, let:

$$\theta = T / T^* , \quad \omega = u / u^* , \quad f = B / B^* ,$$

$$\text{and} \quad \alpha = x / x_c \qquad (A11)$$

where x_c is a characteristic distance determined later. Three dimensionless parameters are also obtained:

$$\beta^* = p^* / (B^{*2} / 2\mu) , \quad R_m^* = u^* B^* / \eta^* j^*$$

$$\text{and} \quad P = w c_p x_c / K_h T^{*5/2} \qquad (A12)$$

where β^* and R_m^* are the plasma-beta and local magnetic Reynolds number at the starred location, and P is essentially a Peclet number based on the characteristic length:

$$x_c = (K_r K_h)^{1/2} T^* / u^* B^* \qquad (A13)$$

which is found by inspection of the normalized equations. This characteristic length is the scale size for a temperature gradient supported by resistive dissipation.

There is an additional scale size for variation due to the change in magnetic field associated with the current density (that drives the dissipation):

$$\frac{dB}{dx} = -\mu j \qquad (A14)$$

$$= -\mu (E^* - uB) / \eta$$

In terms of dimensionless variables, this equation becomes:

$$\frac{df}{d\alpha} = -\Lambda (1 + 1/R_m^* - \omega f) \theta^{3/2} \qquad (A15)$$

where an additional dimensionless parameter is obtained:

$$\Lambda = \mu (K_h / K_r)^{1/2} T^{*5/2} / B^* \qquad (A16)$$

$$= x_c / (\eta^* / \mu u^*)$$

that relates the scale size for thermal conduction balancing resistive dissipation, x_c, to that for which convection balances diffusion of magnetic flux.

Solution of the set of normalized equation is obtained by integrating in the upstream direction from the starred location, where conditions are taken as $f(0) = 1$, $\theta(0) = 1$, and $\Gamma(0) = 0$, ($\Gamma = d\theta/d\alpha$, is a

dimensionless temperature gradient), to insure that uniform conditions are attained in the limit of high magnetic Reynolds number. The actual extent of the flow field is not prescribed, but is determined instead by requirements at the upstream boundary (e.g., necessary heat flux to establish conditions of the entering flow).

For the one-dimensional flow, it is useful to specify a sonic condition at the starred location, rather than providing values for the mass flow that might be inconsistent with such a condition. The necessary value of u^* is then given (in the limit of $R_m^* >> 1$) by:

$$u^{*2} = \gamma RT^* + B^{*2} / \rho^* \mu \qquad (A17)$$

The results of a sample calculation, performed using Mathematica, are displayed in Figures A-1 to A-3. Parameter values are $\Lambda = 2.0$, and $P = 0.1$, for which β^* ($= 2(\gamma - 1)P\Lambda / \gamma$) $= 0.114$. The local value of magnetic Reynolds number is (arbitrarily) $R_m^* = 10$, and the specific heat ratio is $\gamma = 1.4$. Distances are measured upstream of the sonic point by the dimensionless variable $b = x / x_c$.

To return to dimensional quantities, it is necessary to connect the results of the normalized calculation to the conditions of a particular thruster. For example, the heat flux is:

$$q = (K_h T^{*7/2} / x_c) \theta^{5/2} \Gamma \qquad (A18)$$

If the upstream boundary of the flow corresponds to the entry point of cold propellant, the heat flux from the discharge must be sufficient to raise the total enthalpy of this mass to the initial conditions of the discharge flow. For purposes of illustration here, the necessary heat flux may be written as:

$$q_1 = w (Q + c_p T_1 + u_1^2 / 2) \qquad (A19)$$

where Q is the chemical energy per unit mass (including the cost of vaporization, dissociation and ionization), and the subscript '1' refers to the entry station of the flow. The characteristic temperature T^* is then obtained in terms of the chemical energy per unit mass, Q:

$$T^* = (Q / c_p)/[(\theta^{5/2} \Gamma)_1 / P - \theta_1$$
$$- (\gamma - 1)(2 + \gamma\beta^*) \omega_1^2 / 2\gamma\beta^*]$$
$$\qquad (A20)$$

In Fig. A-4, the denominator of Eqn. 21 is displayed for the same parameters previously used. Note that the minimum value of T^* corresponds to $b = 1.6$. For

a Teflon plasma, fully dissociated into singly-ionized constituents, Q is about 62 eV/50 amu, while c_p would be 21 eV/50 amu-eV for the three heavy-particles and three electrons. Thus, $Q/c_p \cong 3$, and the minimum value of T^* is 1.2 eV. Higher temperatures, however, are also possible and would be chosen in order to satisfy other conditions of the thruster, such as the operating value of magnetic field.

The driving source for the thruster can typically be characterized in terms of the current supplied. It is reasonable, therefore, to attempt to specify thruster operation by the magnetic field, B_1, at the entrance of the flow field. The magnetic field at the sonic point is then $B^* = B_1 / f(b_1)$. The temperature at the sonic point is related to the magnetic field by:

$$T^* = \{\Lambda / \mu(K_h / K_r)^{1/2}\}^{2/5} (B_1/f(b_1))^{2/5} \qquad (A21)$$

Consistent solution requires agreement of Eqns. 21 and 22 for a specified magnetic field, B_1. In the present numerical example, this occurs at $b_1 = 1.88$. A total current of 10 kA over a 2 cm width provides a magnetic field of $B_1 = 0.63$ Tesla at the entrance implying (with $f_1 = 1.56$) a value of $B^* = 0.4$ T at the sonic point. For this value, the characteristic temperature may be found in terms of the transport properties of the plasma. (For an ideal, singly-ionized plasma, the values of K_r and K_h are[A1]:

$$K_r = 5.21 \times 10^{-5} \lambda \quad [W\text{-}m\text{-}eV^{3/2}]$$
and $\quad K_h = 7.46 \times 10^4 / \lambda \quad [J / m\text{-}s\text{-}eV^{7/2}]$

where λ is the so-called Coulomb logarithm, and temperatures are measured in eV.) The characteristic temperature (with $\lambda = 10$) is then:

$$T^* = \{ \Lambda B^* / \mu (K_h / K_r)^{1/2} \}^{2/5} \qquad (A22)$$
$$= 7.8 \text{ eV}$$

With the magnetic pressure, and plasma temperature, the mass density at the sonic point can be found in terms of the plasma-beta:

$$\rho^* = \beta^* (B^{*2} / 2\mu) / RT^* \qquad (A23)$$
$$= 8.3 \times 10^{-5} \text{ kg/m}^3$$

The flow speed can also be obtained from the sonic condition in the form:

$$u^{*2} = (B^{*2} / \rho^* \mu) [1 + \gamma\beta^* / 2] \qquad (A24)$$

For the numerical values previously used, $u^* = 41$ km/sec. The characteristic scale-size is 0.93 mm, so the discharge thickness is $d = b_1 x_c = 1.75$ mm.The mass flow per unit area is $\rho^* u^* = 3.4$ kg/m^2-sec. For a cross-sectional area of 4 cm^2, the mass ejected in 10 μs would be 13.6 μg.

Another relationship among parameters:

$$P\Lambda = \mu \rho^* c_p T^* / B^{*2} \qquad \text{(A25)}$$

provides the speed at the sonic point in the form:

$$u^* = Q^{1/2} \{ [1 + {}^\gamma\beta^* /2] / [(\theta^{5/2} \Gamma)_1 / P - \theta_1 - (^\gamma - 1)(2 + {}^\gamma\beta^*) \omega_1^2 / 2^\gamma\beta^*]P\Lambda \}^{1/2}$$

$$\text{(A26)}$$

which displays the basic scaling with Alfven critical speed.

While the numerical results in the present example may be fortuitously close to values observed in various PPT experiments, accurate predictions require modeling based on the actual behavior of the propellant in the full two- (and three-) dimensional, unsteady environment of the thruster.
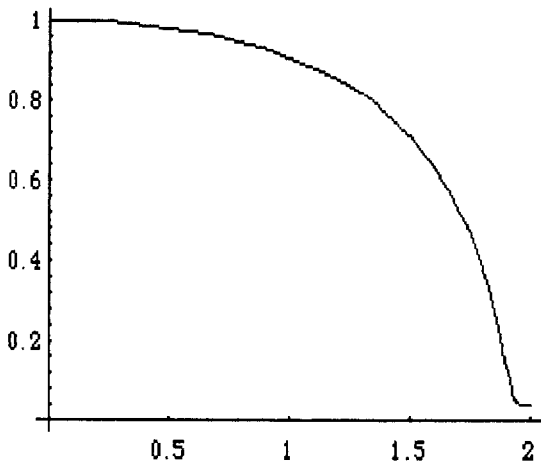
Fig. A-1 Normalized temperature, θ vs normalized distance, b, upstream of sonic point
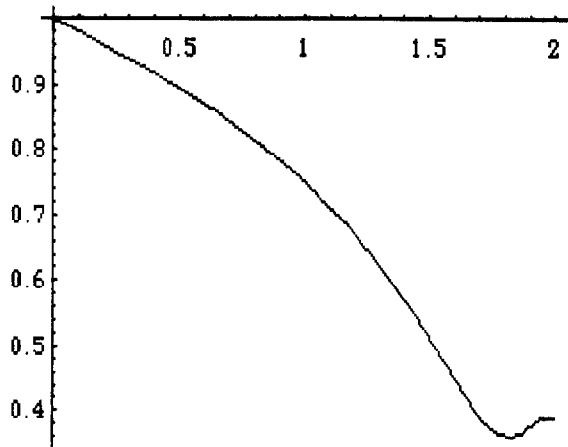
Fig. A-3 Normalized flow speed, ω vs normalized distance, b, upstream of sonic point
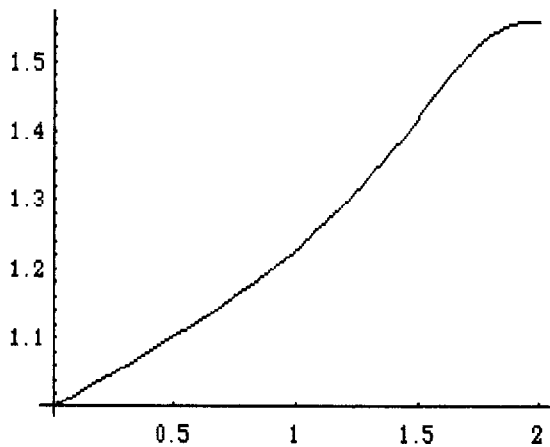
Fig. A-2 Normalized magnetic field, f vs normalized distance, b, upstream of sonic point
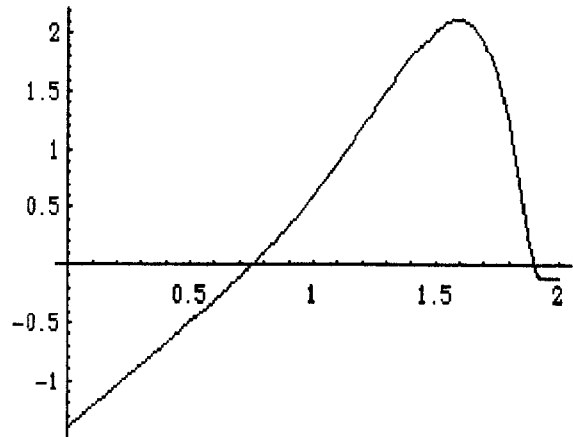
Fig. A-4: $[(\theta^{5/2} \Gamma)_1 / P - \theta_1 - (^\gamma - 1)(2 + {}^\gamma\beta^*) \omega_1^2 / 2^\gamma\beta^*]$ of Eqn. 20 vs normalized distance, b, upstream of sonic point